

A LOOKUP TABLE TO COMPUTE HIGH ENERGY COSMIC RAY  
EFFECTS ON TERRESTRIAL ATMOSPHERIC CHEMISTRY

BY

Dimitra Atri

Submitted to the Department of Physics and Astronomy and the Faculty  
of the Graduate School of the University of Kansas in partial fulfillment of  
the requirements for the degree of Masters of Science

---

Chair: Prof. Adrian L. Melott

---

Prof. Mikhail V. Medvedev

---

Prof. Brian C. Thomas

Date defended: 3 March 2009

The Thesis Committee for Dimitra Atri certifies  
that this is the approved Version of the following thesis:

A LOOKUP TABLE TO COMPUTE HIGH ENERGY COSMIC RAY  
EFFECTS ON TERRESTRIAL ATMOSPHERIC CHEMISTRY

Committee:

---

Chair: Prof. Adrian L. Melott

---

Prof. Mikhail V. Medvedev

---

Prof. Brian C. Thomas

Date approved: \_\_\_\_\_

## ABSTRACT

A variety of events such as gamma-ray bursts and supernovae may expose the Earth to an increased flux of high-energy cosmic rays, with potentially important effects on the biosphere. Existing atmospheric chemistry software does not have the capability of incorporating the effects of substantial cosmic ray flux above 10 *GeV*. An atmospheric code, the NASA-Goddard Space Flight Center two-dimensional (latitude, altitude) time-dependent atmospheric model (NGSFC), is used to study atmospheric chemistry changes. We have created a table that, with the use of the NGSFC code, can be used to simulate the effects of high energy cosmic rays (10 *GeV* - 1 *PeV*) ionizing the atmosphere. By interpolation, the table can be used to generate values for other uses which depend upon atmospheric energy deposition by ensembles of high-energy cosmic rays. We discuss the table, its use, weaknesses, and strengths.

# Contents

<b>1</b>	<b>Introduction</b>	<b>7</b>
<b>2</b>	<b>Methods</b>	<b>9</b>
<b>3</b>	<b>Construction of the Lookup Table</b>	<b>15</b>
<b>4</b>	<b>How to use the lookup table</b>	<b>22</b>
<b>5</b>	<b>Discussion</b>	<b>24</b>

# List of Tables

3.1	Input File for CORSIKA - Complete Description of Variables at [8] . . . . .	20
3.2	Altitudes for NGSFC code. . . . .	21

# List of Figures

2.1	Fractional energy deposition for a 1 TeV primary at $0^\circ$ (solid), $45^\circ$ (dotted), and $70^\circ$ (dashed) per $mb$ (in bins of the NGSFC code) in log pressure, proportional to total column density traversed by the shower, which is approximately linear in altitude.	10
2.2	Electromagnetic energy deposition from a 100 GeV primary (solid), a 10 TeV primary (dotted) and an PeV primary (dashed) per $g\ cm^{-2}$ , in bins of NGSFC code . Energy deposition for the higher energy primaries is deeper in the atmosphere. Energy going into nuclear interactions or hitting the ground is not included in this table . . . . .	14

# Chapter 1

## Introduction

Nearby supernovae [1], gamma ray bursts [2, 3] and possibly galactic shocks [4] may bathe the Earth in cosmic rays (CRs) of much higher than usual incident energies. It is of considerable interest to investigate the effect of such events on the Earth's atmosphere, and consequent possible connections to mass extinctions and other events in the fossil record. In studies of supernovae and gamma ray bursts until now, cosmic rays have been included only by means of a simple phenomenological approximation, enhancing the existing background CR ionization, or not at all. Computations of the effects of gamma-ray bursts [2] have been based on only the effects of photons. However, a sufficiently strong background of very high-energy cosmic rays can punch through the galactic and terrestrial magnetic fields [3] and irradiate the Earth, with effect potentially competitive with those of photons. Other potential scenarios which may account for a 62 My periodicity in biodiversity [4] are based solely on CR, and to date the terrestrial effects have only been approximated. Thus there is considerable value in developing software to model the effects of a spectrum of

CR with energies above those normally included in atmospheric computations.

We have developed a method to model changes in atmospheric chemistry when high energy cosmic rays (HECRs) ionize the atmosphere. When HECRs hit the atmosphere, like other CRs they will interact with atmospheric constituents, primarily the molecules of  $N_2$  and  $O_2$ . This interaction will either result in a nuclear reaction or an ionization reaction, the latter being the interaction of primary importance for chemistry [5]. To study this interaction we created a normalized HECR ionization spectrum data table that contains ionization energy due to HECRs at various energies and altitudes. We will discuss the methods used, how the data table was generated, and its use in a widely used time-dependent atmospheric ionization and chemistry code. This result naturally complements and extends basic work on the lower-energy CRs that normally dominate atmospheric ionization [6].

In order to obtain ionization energy from HECRs, we used CORSIKA (COsmic Ray SIMulations for KAscade), a high energy cosmic ray extensive air shower simulator [7, 8]. The code follows the interactions of a primary cosmic ray and its secondary particles through the atmosphere to the ground. CORSIKA uses Monte Carlo calculations to account for high energy strong and electromagnetic interactions using a number of extensive air shower simulators (of which we used UrQMD-low energy and EPOS-high energy) [9].

Using CORSIKA we created a table so that atmospheric ionization can be calculated for an arbitrary CR spectrum between 10  $GeV$  and 1  $PeV$ . We intend to continuously update this table to higher energies, eventually reaching the highest energies observed.

# Chapter 2

## Methods

The table we have generated gives energy deposition in bins corresponding to those used in the NASA-Goddard two-dimensional atmospheric chemistry code, hereafter NGSFC. However, it can be used for any purpose requiring estimates of energy deposition in the atmosphere by interpolating between those bins.

The NGSFC code has been used extensively to study the effects of supernovae [11], gamma-ray bursts [2] and solar proton events on the atmosphere [10,13]. We will only briefly describe this code, given detailed accounts elsewhere [2, 12, 14]. There are 58 log pressure bands (we use only the first 46 of these bins here, as discussed below) and 18 bands of latitude. The model computes atmospheric constituents with a largely empirical background of solar radiation variations, with photodissociation, and including small scale mixing and winds. Also, it includes an empirical background of CR source ionization based on current levels, which includes an 11-year solar modulation cycle, all with a one day timestep.

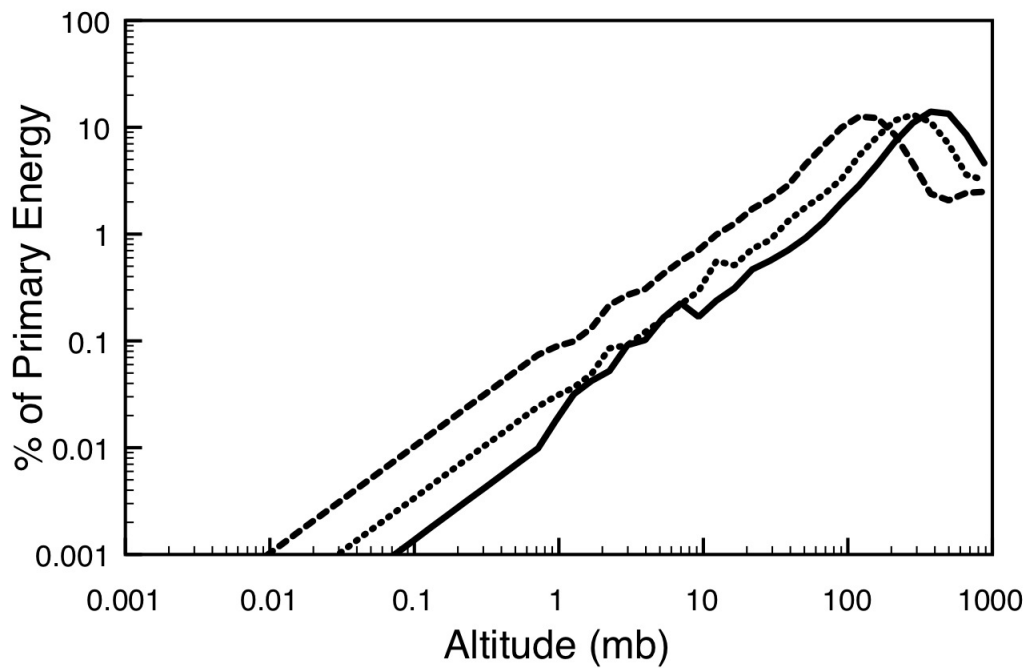


Figure 2.1: Fractional energy deposition for a 1 TeV primary at  $0^\circ$  (solid),  $45^\circ$  (dotted), and  $70^\circ$  (dashed) per  $mb$  (in bins of the NGSFC code) in log pressure, proportional to total column density traversed by the shower, which is approximately linear in altitude.

CRs of  $10^{10} - 10^{15}$  eV are of much larger primary energy than those that dominate normal galactic CRs, so one should not simply turn up the usual background, as in a previous supernova study [11]. We used CORSIKA, which is designed to perform detailed simulations of extensive air showers initiated by high energy cosmic ray particles. We did 25 simulated showers at each of a series of energies by 0.1 in  $\log_{10}$  intervals of primary energy between 10 GeV and 1 PeV, i.e. at 50 different primary energies.

We created a lookup table using data from CORSIKA runs that contains atmospheric ionization energy deposition per primary due to CRs in the range of 10 GeV - 1 PeV. The sum of deposition over altitude is less than the total of the primary energy, as not all energy is deposited in the the atmosphere by electromagnetic processes. Nuclear interactions also occur between HECRs and atmospheric particles, but nuclear energy is dumped into nuclei, mostly not into atmospheric chemistry. Energy that goes into nuclear interactions or reaches the ground is not included in the deposition table.

An arbitrary spectrum can be convolved with this data and the results used in the NGSFC code (or other similar codes) to simulate the effects this energy flux deposition will have on atmospheric chemistry. It is computationally unfeasible at this time to do Monte Carlos over a very large number of angles of incidence. Because of this, we investigated and applied an approximation scheme. We investigated the effect of zenith angle by running 50 shower ensembles (2500 primary particle simulation runs) at zenith angles of  $0^\circ$  (vertical),  $45^\circ$ , and  $70^\circ$  at  $10^{13}$  eV. In Figure 1 we show the fractional energy deposition for each of these zenith angles (excluding nuclear interactions) per

interval (intervals of the NGSFC code) in log pressure, proportional to total column density traversed by the shower, which is approximately linear in altitude. Note that the lateral displacement in the lines, and the location of their maxima, are reasonably approximated by a  $(\cos \theta)^{-1}$  factor, confirming the simplest thing one would expect from a column density factor. For a general-purpose code at the energies we consider, it is appropriate to assume the flux is isotropic. At the level of approximation needed for this assessment of the atmospheric ionization, we replace the ensembles of angles of incidence by a single ensemble at  $\text{arc cos} \langle \sin \theta \cos \theta \rangle$ , where the mean  $\langle \rangle$  is over a hemisphere; this is  $\text{arc cos} (\pi^{-1})$ , or  $71.44^\circ$ . At the level of precision needed for this study, and given the complications in using CORSIKA for greater incidence angles, we have used the  $70^\circ$  ensemble for this purpose. For a non-isotropic source, a column density approximation can be used to adjust the deposition.

For each shower, we recorded the fractional energy deposition in each of 1000 bins of  $1 \text{ g cm}^{-2}$  column density. We used their mean to construct a lookup table describing the energy deposition for a particle of given primary energy as a function of pressure. Below we describe in detail the construction and use of the table.

The greatest deposition of energy per bin corresponds to the first interaction between the incoming CR and the atmosphere, which occurs very high in the atmosphere. Since log column density is nearly linear with altitude, we analyze the maximum energy deposition per bin of log column density. This has weak trends with primary energy, as shown in Figure 2. This gives about 100-200  $\text{g cm}^{-2}$  for  $70^\circ$  zenith angle as the site of the greatest deposition of

energy per unit distance, corresponding to an altitude of about 11-16 *km*. This can be compared with (a) about 13 *km* as the mean altitude of maximal energy deposition density for the normal CR spectrum as implemented in the NGSFC code, strongly biased toward latitudes greater than about 60 degrees, and (b) 22 to 35 *km* as the peak deposition for *keV – MeV* photons, depending upon energy [2,15]. One would expect higher energy CRs to penetrate deeper based on their smaller cross sections. This apparent discrepancy between the altitudes in (a) and our CR data results from the fact that the normal dominant CR spectrum up to about a *GeV*, strongly interacts with the Earth’s magnetic field, comes down with a small zenith angle near the poles, and consequently encounters a lower mean column density than an isotropic ensemble.

The table was originally created to compute ozone ( $O_3$ ) depletion and other atmospheric chemistry changes [5] resulting from energy deposition by HECRs.  $O_3$  lives at altitudes of 10-35 *km* [16] with considerable latitude dependence [15]. Our data is inaccurate from 46-90 *km* because CORSIKA runs on a linear column density scale starting with 1  $g\ cm^{-2}$ , but main effects of atmospheric chemistry changes on the biosphere occur at lower altitudes. A 46-90 *km* altitude is less significant because high-energy CRs rarely have their first interaction that high in the atmosphere.

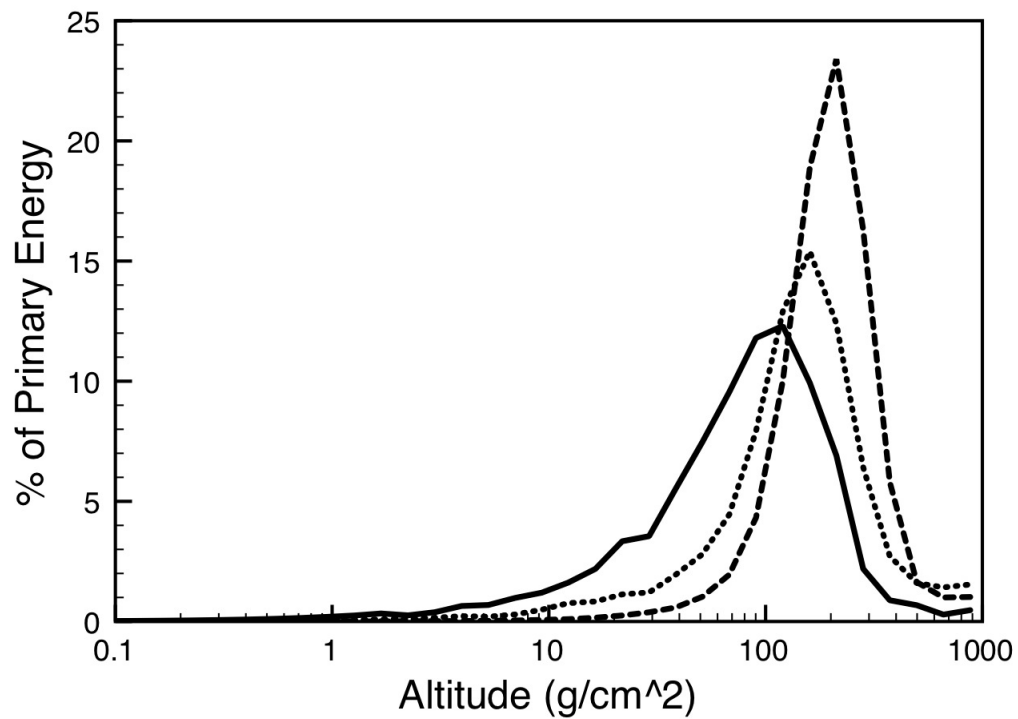


Figure 2.2: Electromagnetic energy deposition from a 100  $GeV$  primary (solid), a 10  $TeV$  primary (dotted) and an  $PeV$  primary (dashed) per  $g\ cm^{-2}$ , in bins of NGSFC code . Energy deposition for the higher energy primaries is deeper in the atmosphere. Energy going into nuclear interactions or hitting the ground is not included in this table

# Chapter 3

## Construction of the Lookup

### Table

The CORSIKA model 6.720 was used in all simulations. When installing CORSIKA, UrQMD was used for the low energy hadronic interaction model and EPOS was used as the high energy hadronic interaction model. None of the extra options were needed here and therefore not installed with CORSIKA. The following are the important variables used in the input file for CORSIKA. The Longitudinal Shower Development variable (LONGI) was set as LONGI T 1 T F giving longitudinal ionization for every  $1 \text{ g cm}^{-2}$  bin. The variable THETAP gives the angle of incidence of particles and was set as THETAP 70 70 as discussed above. The energy range variable (ERANGE) we set as ERANGE x x, where x is the variable energy of the primary particle. CORSIKA was then run 25 times at each of the energies stated above using different SEED random number variables from the input file for each run (Table 1). The data file will output a variety of information. The sum

of the average longitudinal energy deposit in  $GeV$  given at every  $1 g cm^{-2}$  is the only data we are interested in. In the future we plan to extend this table above the  $PeV$  range. Computing time and size of the files for primaries above  $PeV$  range increase approximately linearly with energy. In order to limit these factors within a reasonable range, the thinning algorithm available in CORSIKA will be used when we compute the  $PeV - EeV$  range. When thinning is active, below a fraction (EFRCTHN) of the primary energy, only one of the secondary particles is followed, selected at random according to its energy and the rest of the secondaries are discarded. An appropriate weight (WMAX) is attached to the surviving particle to conserve energy. Parameter RMAX is the radius within which all particles are subjected to inner radius thinning. The following values of the thinning parameters, EFRCTHN = 1.E-5, WMAX = 1.E5 and RMAX = 3.E4, THINRAT = 1.E0, WEITRAT = 1.E2, produced reasonable data quality keeping the computing time and size of the data files within acceptable range. The following lines will be added to the CORSIKA input file for primary energy  $>1 PeV$ : THIN 1.000E-05 1.000E+05 3.000E+04 and THINH 1.000E+00 1.000E+02.

CORSIKA ran at 50 different energy levels 25 times each at intervals of 0.1 in log energy. Each time it was run CORSIKA simulated 15 protons entering the atmosphere. Therefore, we compiled 375 particles for each of the 50 energy levels. The energy was averaged linearly for each of the 25 runs at each longitudinal pressure bin.

Minor problems arose when transferring the CORSIKA data to the NGSFC code. First, the lowest column density at which energy deposition is given

is  $1 \text{ g cm}^{-2}$  in CORSIKA, while 22 of the 46 pressure levels are below  $1 \text{ g cm}^{-2}$  in the NGSFC code. Secondly, CORSIKA outputs deposition in a linear pressure scale. We interpolated to a logarithmic scale for the NGSFC code. We converted CORSIKA density units of  $\text{g cm}^{-2}$  to millibars (needed for NGSFC) by a conversion factor of 0.98.

To resolve the problem of CORSIKA's highest interaction altitude being below 22 of the NGSFC codes altitudes we linearly interpolated the data using the ionization from the  $1 \text{ g cm}^{-2}$  bin. Because the first interaction point of primaries is rarely within the first  $\text{g cm}^{-2}$ , most of the CORSIKA output files have no energy deposition for this altitude. Also, the data we used from CORSIKA is binned in  $0.1 \text{ GeV}$  intervals, meaning for the lower energy runs many of the 1036 altitude levels are zero. For this reason our output file may have no energy in the 22 highest altitude bins for certain energy levels. For our purpose of looking at the ozone these higher altitudes, above  $\sim 46 \text{ km}$ , are not important, since the amount of ionization in them from HECR would be quite small.

We use the same linear interpolation method used for each bin with less than  $1 \text{ g cm}^{-2}$ , depositing the energy from ground level to the highest logarithmic altitude level in the last bin. The logarithmic altitude bins are centered on the bins used in the NGSFC code (Table 2).

The geomagnetic field should be mentioned with regard to the lookup table. Its impact on CRs is minor for protons with energies greater than  $17 \text{ GeV}$  [17]. Because this only impacts a small region of the CR range of importance ( $10 \text{ GeV} - 1 \text{ EeV}$ ) effects due to the magnetic field are small. If desired, alterations

to the latitude distribution of energy deposition can be made in the 10 to 17  $GeV$  range to simulate the effects of deflection by the geomagnetic field.

Name	Value	Description
RUNNR	x	run number x = integer number to help keep track of runs
NSHOW	15	number of showers to generate
PRMPAR	14	Primary Particle, 14 = proton
ESLOPE	-2.7	slope of primary energy spectrum (irrelevant in our model because we use single energy level)
ERANGE	X X	Energy range of particle (GeV) X = Energy of Particle (Table 2)
THETAP	70 70	range of zenith angle (degree)
PHIP	-180. 180.	range of azimuth angle (degree)
SEED	x 0 0	random number sequence 1
SEED	x 0 0	random number sequence 2
OBSLEV	0.	Observation level (cm)
ECUTS	.3 .3 .00005 .00005	Energy to cut off secondaries
MAGNET	20.0 42.8	Magnetic field centr. Eurpoe
HADFLG	0 0 0 0 0 2	Flags hadr interact & fragmentation
MUADDI	T	Additional infor for muons
MUMULT	T	Muon multiple scattering
ELMFLG	F T	em. interaction flags (NKG,EGS)
STEPFC	1.0	mult. scattering step length fact.
RADNKG	200.E2	outer radius for NKG lat.dens.distr.

ARRANG	0.	rotation of array to north
MUADDI	T	Additional muon information
LONGI	T 1 T F	V step 10
EPOPAR	input ../epos/epos.param	initialization input file for epos
EPOPAR	fname inics ../epos/epos.inics	initialization input file for epos
EPOPAR	fname iniev ../epos/epos.iniev	initialization input file for epos
EPOPAR	fname initl ../epos/epos.initl	initialization input file for epos
EPOPAR	fname inirj ../epos/epos.inirj	initialization input file for epos
EPOPAR	fname inihy ../epos/epos.ini1b	initialization input file for epos
EPOPAR	fname check none	dummy output file for epos
EPOPAR	fname histo none	dummy output file for epos
EPOPAR	fname data none	dummy output file for epos
EPOPAR	fname copy none	dummy output file for epos
ECTMAP	1.E2	Cut on gamma factor for printout
MAXPRT	5	Max. number of printed events
DIRECT	/data/dimitra/	Output directory
DATBAS	F	Write .dbase file
USER	you	User
PAROUT	F F	
DEBUG	F 6 F 1000000	Debug flag and log unit for out
EXIT		End input file

Table 3.1: Input File for CORSIKA - Complete Description of Variables at [8]

Number of Bin	Pressure (mb)	Approximate Altitude (km)
1	879	0
2	661	2
3	498	4
4	374	6
5	282	8
6	212	10
7	160	12
8	120	14
9	90.3	16
10	68.0	18
11	51.1	20
12	38.5	22
13	29.0	24
14	22.8	26
15	16.4	28
16	12.3	30
17	9.28	32
18	6.98	34
19	5.26	36
20	3.96	38
21	2.98	40
22	2.24	42
23	1.68	44
24	1.27	46
25	0.954	48
26	0.718	50
27	0.540	52
28	0.406	54
29	0.306	56
30	0.230	58
31	0.173	60
32	0.130	62
33	0.0980	64
34	0.0738	66
35	0.0555	68
36	0.0418	70
37	0.0314	72
38	0.0237	74
39	0.0178	76
40	0.0134	78
41	0.0101	80
42	0.00758	82
43	0.00571	84
44	0.00429	86
45	0.003230	88
46	0.002430	90

Table 3.2: Altitudes for NGSFC code.

# Chapter 4

## How to use the lookup table

The lookup table is formatted into 50 columns and 46 rows corresponding to the primary energy of the particle and the altitude bins of the NGSFC code, respectively. As is, it displays ionization energy deposition for a spectrum of 1 particle for every 0.1 logarithmic energy bin, or 1 particle at each of the 50 energies, in units of *GeV*. Trivially, one must multiply by the number of particles per unit area per second in their bin to get the total energy flux at each altitude bin for a given spectral form. From this point the procedure may vary depending on the use to which the lookup table is put. To input this data into the NGSFC code the energy at each altitude must be added over all energy levels, creating a 1-dimensional data set of total energy deposition flux at each altitude.

As mentioned previously, the NGSFC code takes ionization energy flux in a 2-dimensional format using altitude and latitude. The data is now in 1-dimension with respect to altitude, so the user must create a latitude component. The NGSFC code has 18 latitude bins ( $90^\circ - 80^\circ$ ,  $80^\circ - 70^\circ$ ,  $70^\circ - 60^\circ$

etc). For an isotropic flux, the same flux is entered for each latitude bin. The final data file to be input into the NGSFC code should now be a 2-dimensional set of ionization energy flux deposition at the 18 latitude bins for 46 altitudes, a total of 828 data points. For a point source, the input into latitude bins may be adjusted by the appropriate factor, including a correction for the  $\cos \theta$  factor as in [2]. This may result in hemispheric differences in the results.

The energy flux data as a function of altitude and latitude, generated as described above, may be used in the NGSFC code by way of a simple read-in subroutine. Depending on the units of the spectrum used, conversion to  $cm^{-2}s^{-1}$  may be necessary since the NGSFC code uses *cgs* units. In order to use the input as a source of  $NO_y$ , the energy flux must first be converted to ionization flux. This is accomplished using 35 *eV* per ion pair [18], which finally gives values in units of *ions cm<sup>-2</sup>s<sup>-1</sup>*. Constituents in the code are stored with units of number *cm<sup>-3</sup>s<sup>-1</sup>*. Therefore, the area ionization rate is converted to a volume rate using the height of the altitude bins, which depends on the current density of each bin at read in (the density depends on temperature, which depends on the presence of sunlight, etc.). This ionization rate is then used as a source for  $NO_y$ , assuming 1.25 molecules are created for each ion pair [16]. The model then runs as usual, incorporating this source of  $NO_y$  in the relevant chemistry computations. The general procedure here is the same as that used in previous work with both photon and solar proton ionization sources [2, 10].

# Chapter 5

## Discussion

Since the Sun is a major source of atmospheric ionization on earth, the atmospheric ionization studies until now have been focussed on solar cosmic rays which fall in the lower energy part of the observed cosmic ray spectrum. There are other phenomena, such as supernovae, gamma-ray bursts and the periodic motion of the earth perpendicular to the plane of our galaxy, which have a potential to expose the Earth to a flux of high energy cosmic rays. A study of the effects of such phenomena on the Earth's atmosphere is not possible based on atmospheric ionization work done on lower energy cosmic rays.

We have not only produced ionization data for high energy cosmic rays, but have also interfaced this data to run with the photochemical code (NASA GSFC 2D Atmospheric Modeling code) to compute changes in atmospheric chemistry. We found that as we go higher in energy, particles penetrate deeper, as expected from the cross sections. As a result, we see enhanced ionization near the ground for higher energies.

Our data can also be interpolated to any other format suited for that par-

ticular model to explore other effects caused due to atmospheric ionization. We plan to extend our results up to the highest energies observed. Also, the inclusion of CR effects will make possible a more accurate investigation of the effects of gamma-ray bursts on the Earth, which have the potential to explain certain mass extinction events [19]. A quantitative treatment of possible time-varying flux of high-energy CRs becomes possible [5]. It may have other applications which we cannot anticipate, and should be made generally available.

This lookup table will be made freely available via ftp, and upgraded in the future as appropriate.

Look for a link at *[http : //kusmos.phsx.ku.edu/ ~ melott/Astrobiology.htm](http://kusmos.phsx.ku.edu/~melott/Astrobiology.htm)*.

# Bibliography

- [1] B.D. Fields, T. Athanassiadou, and S.R. Johnson, *Supernova Collisions with the Heliosphere*, *Astrophys. J.* **678**, 549 (2008).
- [2] B.C. Thomas, A.L. Melott, C.H. Jackman, C.M. Laird, M.V. Medvedev, R.S. Stolarski, N. Gehrels, J.K. Cannizzo, D.P. Hogan, and L.M. Ejzak, *Gamma-Ray Bursts and the Earth: Exploration of Atmospheric, Biological, Climatic, and Biogeochemical Effects*, *Astrophys. J.* **634**, 509 (2005).
- [3] C.D. Dermer and J.M. Holmes, *Cosmic Rays from Gamma-Ray Bursts in the Galaxy*, *Astrophys. J.* **628**, L21 (2005).
- [4] M.M. Medvedev and A.L. Melott, *Do Extragalactic Cosmic Rays Induce Cycles in Fossil Diversity?*, *Astrophys. J.* **664**, 879 (2007).
- [5] A.L. Melott, A.J. Krejci, B.C. Thomas, M.V. Medvedev, G.W. Wilson, and M.J. Murray, *Atmospheric consequences of cosmic-ray variability in the extragalactic shock model*, *J. Geophys. Res.* **113**, E10007, doi:10.1029/2008JE003206 (2008).

- [6] I.G. Usoskin and G.A. Kovaltsov, *Cosmic ray induced ionization in the atmosphere: Full modeling and practical applications*, *J. Geophys. Res.* **111**, D21206, doi:10.1029/2006JD007150 (2006).
- [7] T. Djemil, R. Attallah, and J. N Capdevielle, *Simulation of the Atmospheric Muon Flux with Corsika*, *Int. J. Mod. Phys. A* **20** 6950 (2005).
- [8] T. Pierog, D. Heck, and J. Knapp, <http://www-ik.fzk.de/corsika/>.
- [9] T. Pierog, R. Engel, D. Heck, S. Ostapchenko, and K. Werner, Prepared for 30th International Cosmic Ray Conference, *Latest Results from the Air Shower Simulation Programs CORSIKA and CONEX, (ICRC 2007)*, Merida, Yucatan, Mexico, arXiv:0802.1262v1 (2007).
- [10] C.H. Jackman and R.D. McPeters, *The Effect of Solar Proton Events on Ozone and Other Constituents*, *Geophys. Monogr. Ser.* edited by J.M. Pap and P. Fox, **141**, 305 (2004).
- [11] N. Gehrels, C. M. Laird, C. H. Jackman, J. K. Cannizzo, B. J. Mattson, C. Wan, *Ozone depletion from nearby supernovae*, *Astrophys J.* **585**, 1169 (2003).
- [12] C.H. Jackman, M.T. DeLand, G.J. Labow, E.L. Fleming, D.K. Weisenstein, M.K.W. Ko, M. Sinnhuber, and J.M. Russell, *Neutral atmospheric influences of the solar proton events in October/November 2003*, *J. Geophys. Res.* **110**, A09S27, doi: 10.0129/2004JA010888 (2005).

- [13] B.C. Thomas, C.H. Jackman, and A.L. Melott, *Modeling atmospheric effects of the September 1859 solar flare*, *Geophys. Res. Lett.* **34**, L06810, doi:10.1029/2006GL029174, (2007)
- [14] C.H. Jackman, E.L. Fleming, S. Chandra, D.B. Considine, J.E. Rosenfield, *Past, present, and future modeled ozone trends with comparisons to observed trends*, *J. Geophys. Res.* **101**, 28,753 (1996).
- [15] L.M. Ejzak, A.L. Melott, M.V. Medvedev, and B.C. Thomas, *Terrestrial Consequences of Spectral and Temporal Variability in Ionizing Photon Events*, *Astrophys. J.* **654**, 373 (2007).
- [16] M.B. Harfoot, D. J. Beerling, B. H. Lomax, and J. A. Pyle, *A two-dimensional atmospheric chemistry modeling investigation of Earth's Phanerozoic O<sub>3</sub> and near-surface ultraviolet radiation history*, *J. Geophys. Res.* **112** D07308 (2007), doi:10.1029/2006JD007372.
- [17] <http://www.cosmicrays.org/muon-cutoff-rigidity.php>
- [18] H.S. Porter, C.H. Jackman, A.E.S. Green, *Efficiencies for production of atomic nitrogen and oxygen by relativistic proton impact in air*, *J. Chem. Phys.* **65**, 154 (1976).
- [19] A.L. Melott and B.C. Thomas, *Late Ordovician geographic patterns of extinction compared with simulations of astrophysical ionizing radiation damage*, *Paleobiology*, **35**, 311-320 (2009)